6.1 Introduction

Viscoelastic solutions have received considerable attention due to their application as drag coefficient reducers and as fracturing fluids in enhanced oil recovery [1, 2]. According to the generally agreed upon model [3], the viscoelastic effect arises due to the formation of elongated rod shaped micelles, and the resulting a gel-like structure in solutions. There is no clear explanation exists as why the viscoelastic effect presents only in few surfactant systems. However, various studies show that viscoelasticity can be correlated with certain factors such as packing constraints, ionic strength, nature of headgroup or chain length of the surfactant.

Micelles can undergo transition from spherical – to – rod like under appropriate conditions of salinity, temperature or addition of some organic counterions. Elongated micelles of alkyltrimethylammonium and alkylpyridinium bromides are typical examples and have been investigated in detail by various physico-chemical methods. This feature has been observed more specifically in presence of above cationic surfactants solutions having specific organic counterions such as salicylate, 3-hydroxy- 2-naphthalene carboxylate, alkyl sulfonate, anthranilate etc.[4-10]. Recently, viscoelsticity has also been observed with cationic gemini surfactants in presence of organic salts [11-13].

A counterion mediated micellar growth study suggests that aromatic counterions are more effective in penetrating the headgroup region in comparison to inorganic counterions. This leads to micellar growth at lower [organic salt]. The formation of rodlike micelles is attributed to the strong binding of organic counterions to cationic micelles to minimize the contact of their bulky hydrophobic part with water. The bound counterions reduce the electrostatic repulsion between the cationic headgroups and also facilitate simultaneously the hydrophobic interactions. This results in tighter packing, modifying the spontaneous curvature of the surfactant assemblies and the solution properties [14,15].

Much less is known in comparison to cationic surfactant, regarding the ability of anionic surfactants to form grown or rod like micelles. SDS (an anionic surfactant) is

a power house in academic and industrial research fields. However, only a few studies are available on the micellar growth behavior of SDS in presence of various additives [16-24].

Therefore, it is of great importance to study the micellar growth behavior of anionic surfactants in presence of various additives. Hence we focused on the growth of anionic micelles in water as a function of [additive] and nature of the headgroup. It has been reported that micellar growth (or viscoelasticity) can only be produced when the additive solubilizes at / in certain solubilization site of the micelle [25].

Ample examples are available in the literature to illustrate that a combination of viscosity, NMR and DLS can be used to study micellar morphology and for probing the location and orientation of the molecules in and around a micelle [10, 11, 13, 25, 27-30].

Effect of additions of aromatic salts / drugs namely ANHC, PTHC, TBAB, AMT and PMZ to anionic surfactant (SDS and SDST) solutions have been studied using various physico-chemical techniques. Viscosity measurements helped in deciding the various samples for NMR or DLS measurements.

6.2 Results and discussion

Viscosity, ^{1}H NMR spectroscopy and DLS are the convenient methods for the simultaneous monitoring of changes in aggregate morphology. Surfactant solutions containing spherical micelles are isotropic in nature and of low viscosity [31], whereas the presence of rod-shaped micelles imparts higher viscosity to the solution [3, 32]. Thus, viscosity can be used to study structural transitions in the surfactant solutions (s $\rightarrow$ r). The shape of the micelles whether they are spherical or rod-like, must be decided by a balance between the repulsive electrostatic forces of the headgroups and the attractive forces that cause aggregation. Ample examples exist in the literature to illustrate that ^{1}H NMR spectroscopy can be used to probe the location and orientation of the molecules in and around a micelle by means of the chemical shift, line width and line shape changes observed for the surfactant resonances [26, 27, 28].

Figure 1 shows the variation of η_r of aqueous 30 mM anionic surfactant (SDS or SDST) solutions with different concentrations of ANHC at 30 ˚C. The value of η_r remains nearly constant with a initial increase in [ANHC] with both the surfactants. However, after a certain [ANHC], a gradual increase in η_r is observed with SDS while a precipitation (without any increase in η_r) is observed with SDST. ANHC would furnish a ANH^+ cation which can interact with negatively charged SDS micelles electrostatically and hydrophobically (see Scheme1 of chapter 2). The hydrophobic portion of ANH^+ may facilitate intercalation of this ion between the anionic headgroups of similar charge. These interactions would decrease a_0 and increase effective *v*. The variations in a_0 and *v* would be responsible for the increase in R_p. It is known that increase in R_p is responsible for the formation of higher order aggregates (micellar growth). This micellar growth in SDS solution due to the presence of ANHC is responsible for the increase in η_r as observed in Figure 1. Surprisingly this effect is absent with SDST-ANHC system. It means that ANHC is failed to induce micellar growth in SDST solution. It has been reported that *cmc* is lower in case of SDS than SDST [33]. α also depends on the surface charge density of the micelle. Greater surface charge density (smaller will be the a_0) causes higher α. Also, a_0 is lower for SDS headgroup (0.52 nm^2) than the SDST (0.56 nm^2). Above difference seems responsible for the viscosity behavior depicted in Figure 1.

Figure 2 shows the variation of η_r, for both the surfactants, with the addition of PTHC. The behavior was similar (though some η_r changes can be seen) with SDST as observed in case of ANHC. However, η_r changes are remarkable with SDS-PTHC. This is possibly due to the difference in microenvironment felt by the additive near the head group region. The increased micellar growth in case of PTHC (than ANHC) may be due to the additional methyl group (at para position). It provides extra hydrophobicity which causes increased hydrophobic interactions in addition to the usual electrostatic interaction. It has been reported earlier that substitution of methyl group by ethyl group causes increased micellar growth when the alkyl substituted organic salts were added to a cationic surfactant [34]. However, an insignificant change in viscosity was observed when another organic salt (TBAB) was added in

solution of SDS or SDST (Figure 3). Presence of TBAB does not change micellar shape and hence no change in viscosity is observed.

Both surfactants show an increase in η_r with the addition of AMT and PMZ (both are antidepressant drugs) after a certain concentration (Figures 4 and 5). The η_r variation is similar like SDS-ANHC / PTHC. The results indicate that the micellar growth is facilitated at lower [drug] compared to that of ANHC/PTHC. However, AMT showed better viscosity increase with SDS than SDST (Figure 4). Both the drugs contain tricyclic portion (hydrophobic) and tertiary amine portion (hydrophilic). Both the surfactants showed similar viscosity behavior with a earlier rise in case of SDS. However, precipitation occurs before any distinct viscosity rise with SDS-PMZ system. To our surprise, SDST showed a significant increase in viscosity at higher [PMZ]. Probably, lower molecular area of PMZ [35] allows it to penetrate better into SDST micelles and responsible for increased hydrophobic interactions. Above interrelated factors seem responsible for better performance of SDST in increasing viscosity of the solution as well as for micellar growth

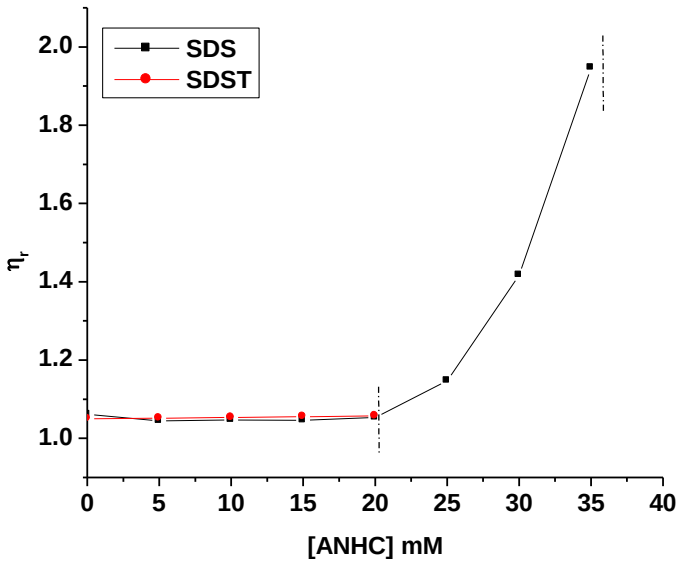

Figure 1 Variation of η_r of aqueous 30 mM surfactant with different concentrations of ANHC at 30 ˚C (up to the solubility limit indicated by dotted lines).

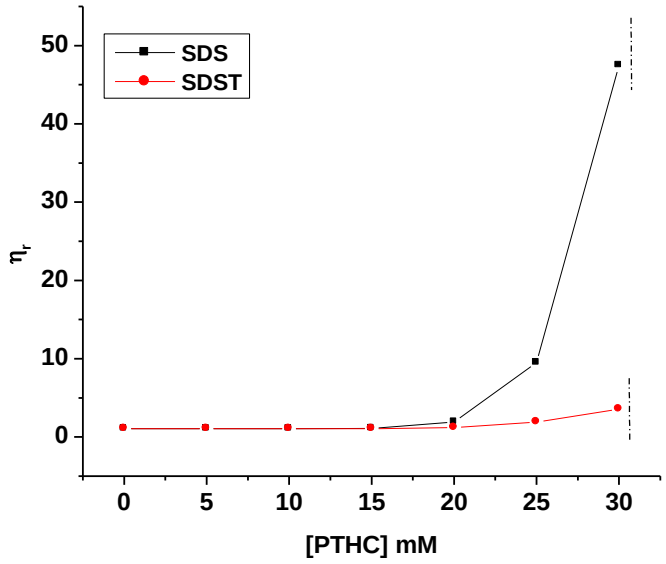

Figure 2 Variation of η_r of aqueous 30 mM surfactant with different concentrations of PTHC at 30 ˚C (up to the solubility limit indicated by dotted lines).

.

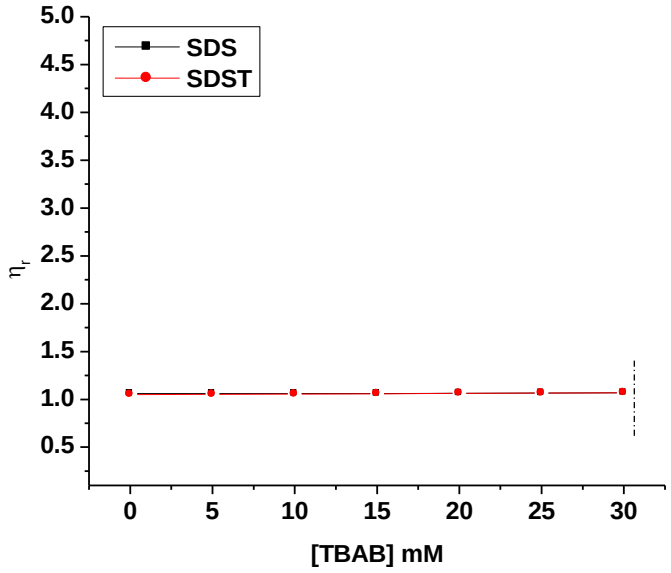

Figure 3 Variation of η_r of aqueous 30 mM surfactant with different concentration of TBAB at 30 ˚ C (up to the solubility limit indicated by dotted lines).

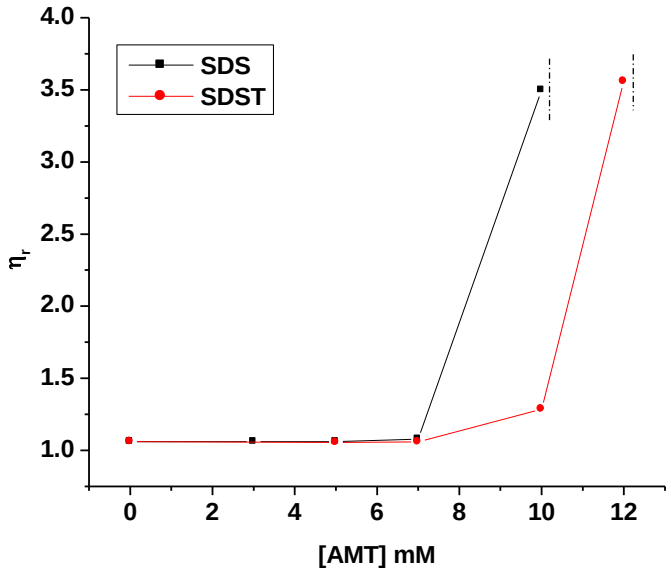

Figure 4 Variation of η_r of aqueous 30 mM surfactant with different concentrations of AMT at 30 ˚ C (up to the solubility limit indicated by dotted lines).

.

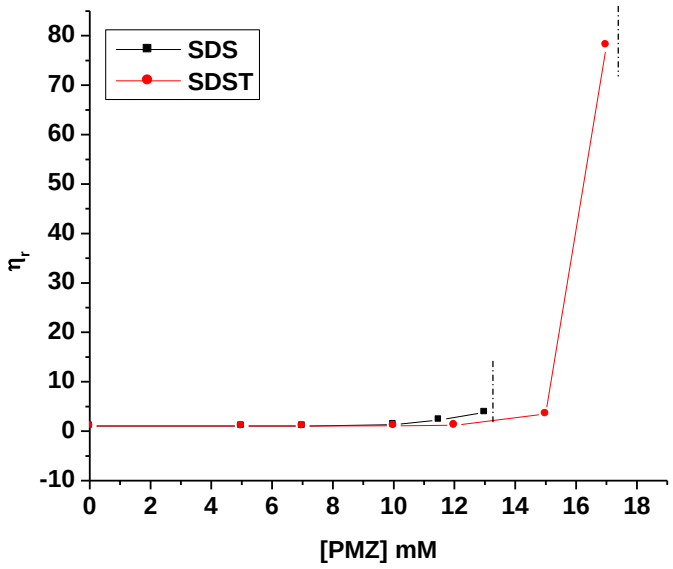

Figure 5 Variation of η_r of aqueous 30 mM surfactant with different concentrations of PMZ at 30 ˚ C.

6.2.1 Variation of proton microenvironment upon interaction between surfactants and salts

The surfactant concentration used is 30 mM, which is about three times larger as than *cmcs*. Therefore, the observed δ basically reflect the protons of the surfactant molecules in the aggregates (Figures 6 and 7). The hydrophobic moieties of the surfactants near the core of the micelles are highly shielded and therefore show resonances at low δ values. However, as we move toward the headgroup ($-SO_4^{-1}$/ $-SO_3^{-1}$) the presence of polar environment makes the adjacent protons more deshielded and, therefore, shows higher δ values. ^{1}H NMR spectra for pure ANHC, PTHC, TBAB, AMT and PMZ are shown in Figures 8, 9, 10, 11 and 12.

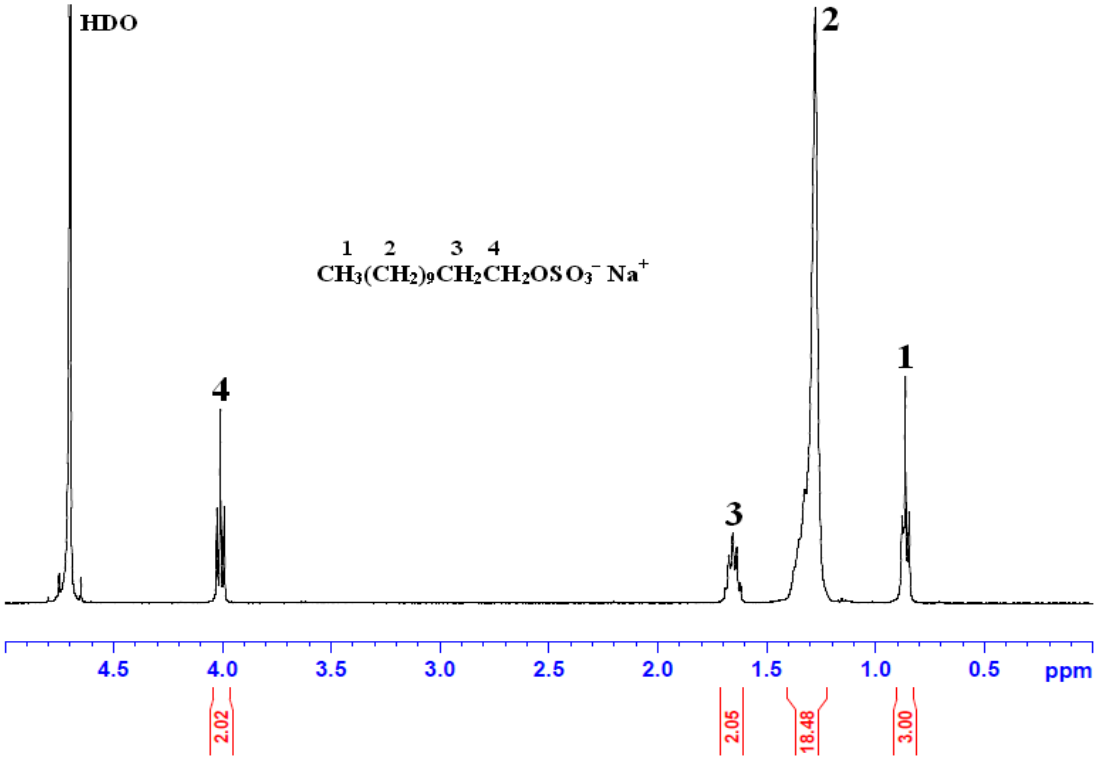

Figure 6 400 MHz ^{1}H NMR spectrum of 30 mM SDS in D_2O at 30 ˚C.

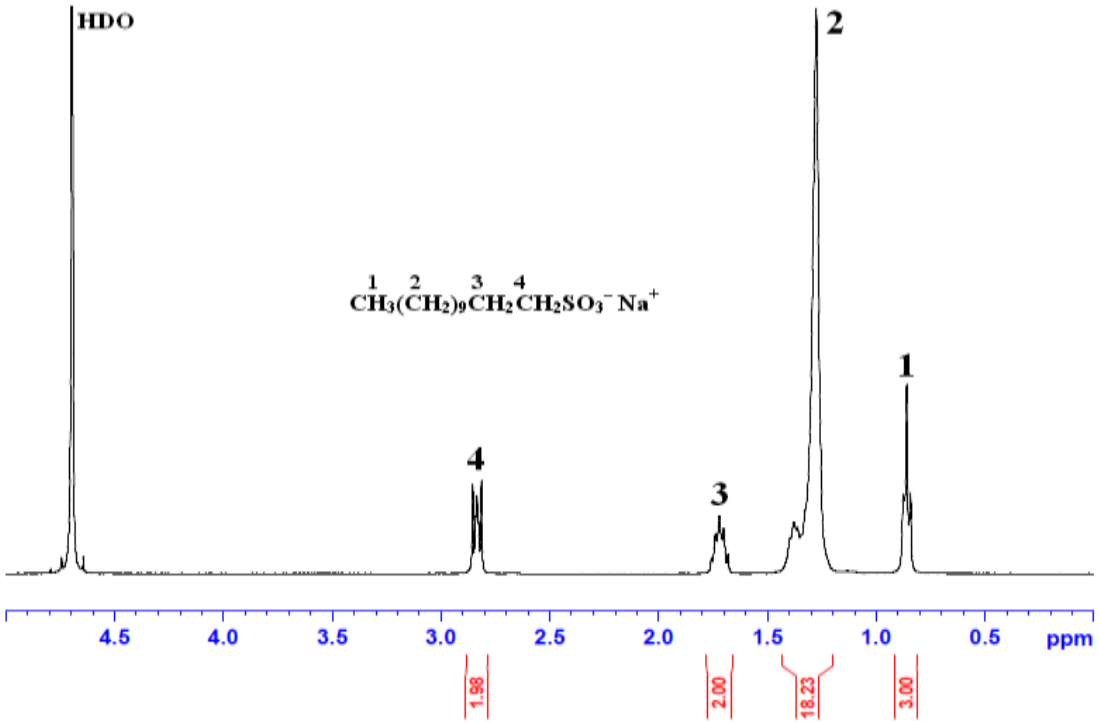

Figure 7 400 MHz ^{1}H NMR spectrum of 30 mM SDST in D_2O at 30 ˚C.

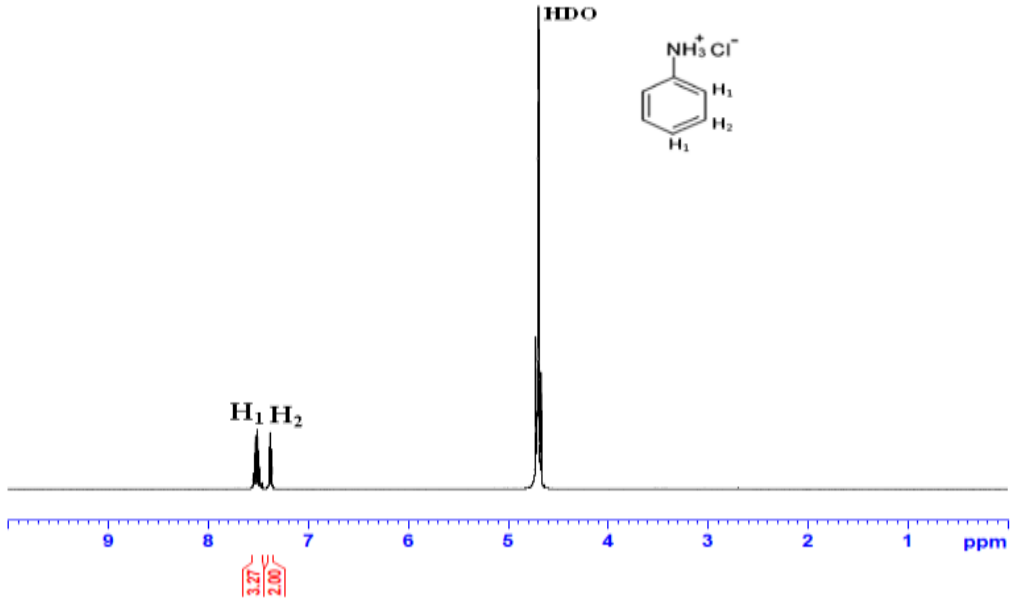

Figure 8 400 MHz ^{1}H NMR spectrum of ANHC in D_2O at 30 ˚C.

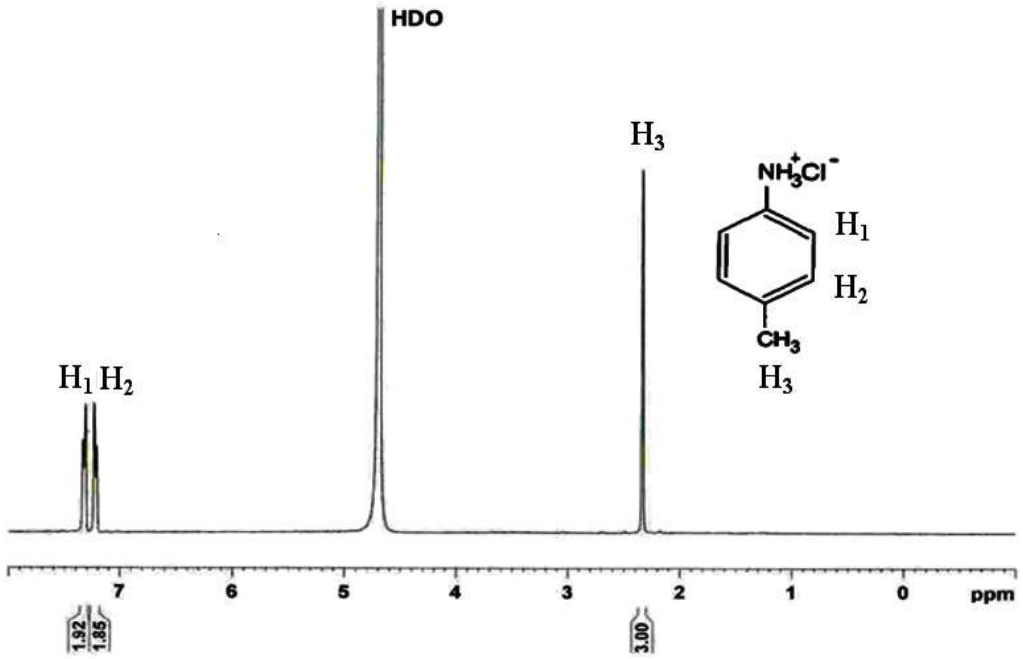

Figure 9 400 MHz ^{1}H NMR spectrum of PTHC in D_2O at 30 ˚C.

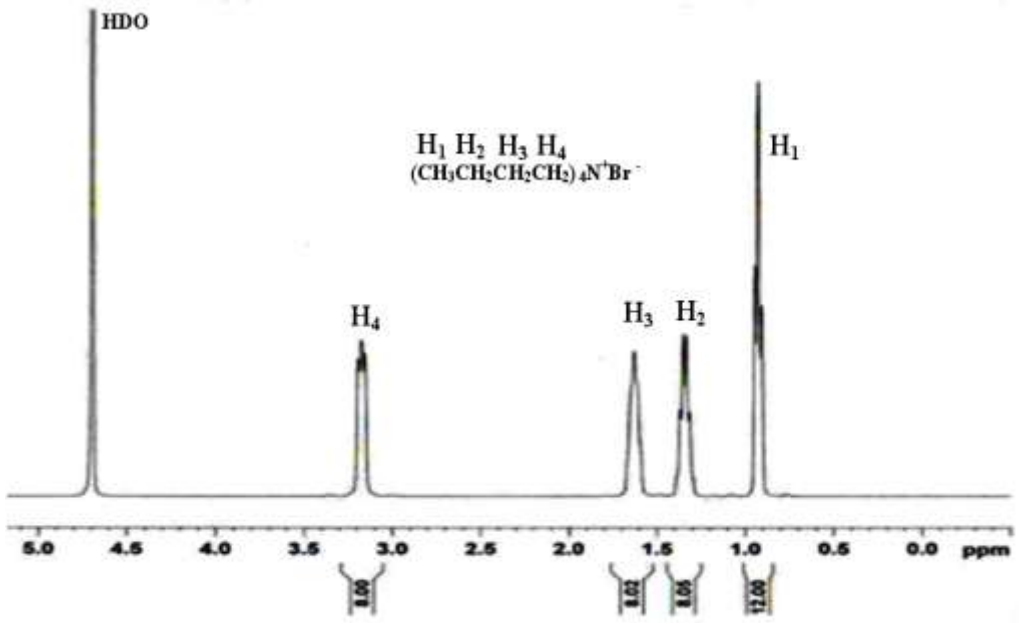

Figure 10 400 MHz ^{1}H NMR spectrum of TBAB in D_2O at 30 ˚C.

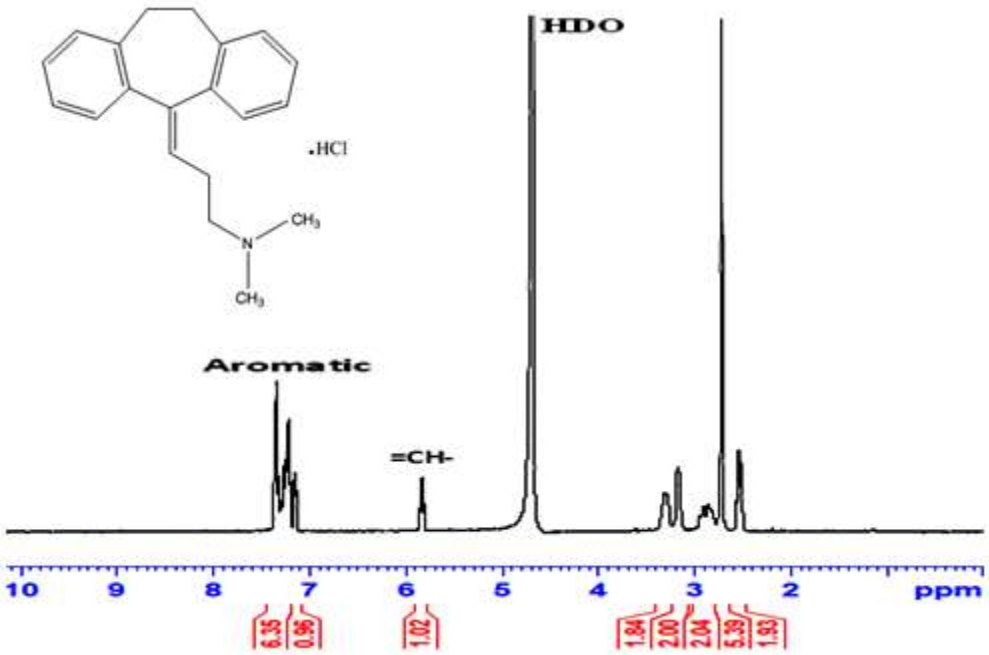

Figure 11 400 MHz ^{1}H NMR spectrum of AMT in D_2O at 30 ˚C.

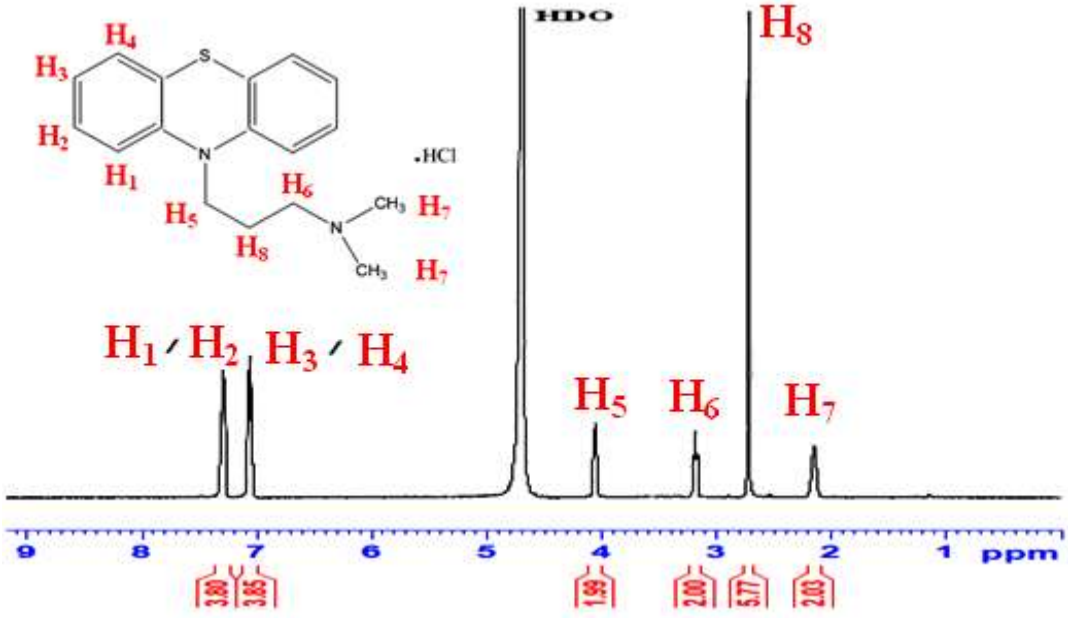

Figure 12 400 MHz ^{1}H NMR spectrum of PMZ in D_2O at 30 ˚C.

^{1}H NMR spectra of 30 mM SDST and SDS with different concentrations of ANHC are shown in Figures 13 and 14. The NMR data show that ANHC is effective to change various proton peaks in case of SDS. However, SDST peaks more or less remained same on addition of ANHC. The NMR data, therefore, show similar trend as observed by viscosity measurements (Figure 1). Chemical shift and line broadening of all protons (except 1-H) on addition of ANHC to aqueous SDS indicate that micelles are growing on addition of ANHC as proposed by viscosity measurements. The probable reason of the peak broadening and disappearance is that the motion of the surfactant molecules is highly restricted in the higher order aggregates [36, 37]. When micellar growth (spherical to rod-like micelles) takes place fast local motion of the segments accompanying growth of the local order in the process of rod-shaped micelle formation slow down because of increase in the intramolecular magnetic dipole-dipole interaction. The growth of the more organized assembly promotes the relaxation rate (reduce) due to the slower motions of the chains (*e.g.* segmental motions or rotations of the rod-like micelles as a whole), thereby broadening of the peak take place. Therefore, broadening of the peak has been interpreted in terms of morphological transition from sphere-to-rod like micelles [38]. Similar line broadening has been reported for ionic surfactants on addition of variety of salts and explained in the light of sphere to rod transition or micellar growth [11, 13, 38, 39]. The peak broadening has been found significant for PTHC with both the surfactants (Figures 15 and 16). However, proton peaks of SDS (Figure 16) are found broader as well as a few peaks are either merged or disappeared (due to broadening). It may be mentioned here that NMR peaks of both the surfactants are nearly unaffected in presence of TBAB (Figures 17 and 18)

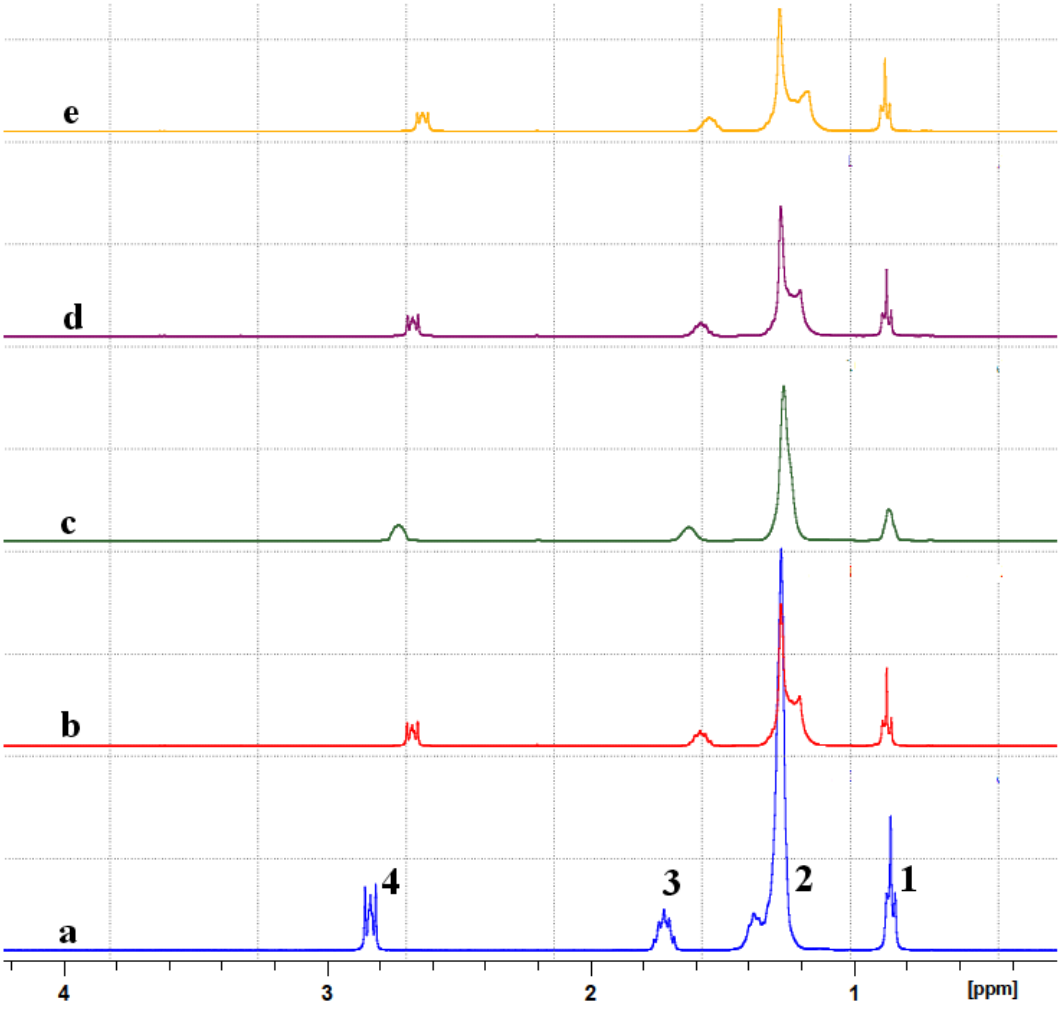

Figure 13 ^{1}H NMR spectra of aqueous 30 mM SDST with various [ANHC] (a) pure 30 mM SDST (b) 30 mM SDST + 5 mM ANHC (c) 30 mM SDST + 10 mM ANHC (d) 30 mM SDST + 15 mM ANHC (e) 30 mM SDST + 20 mM ANHC at 30 $^{\circ}$C.

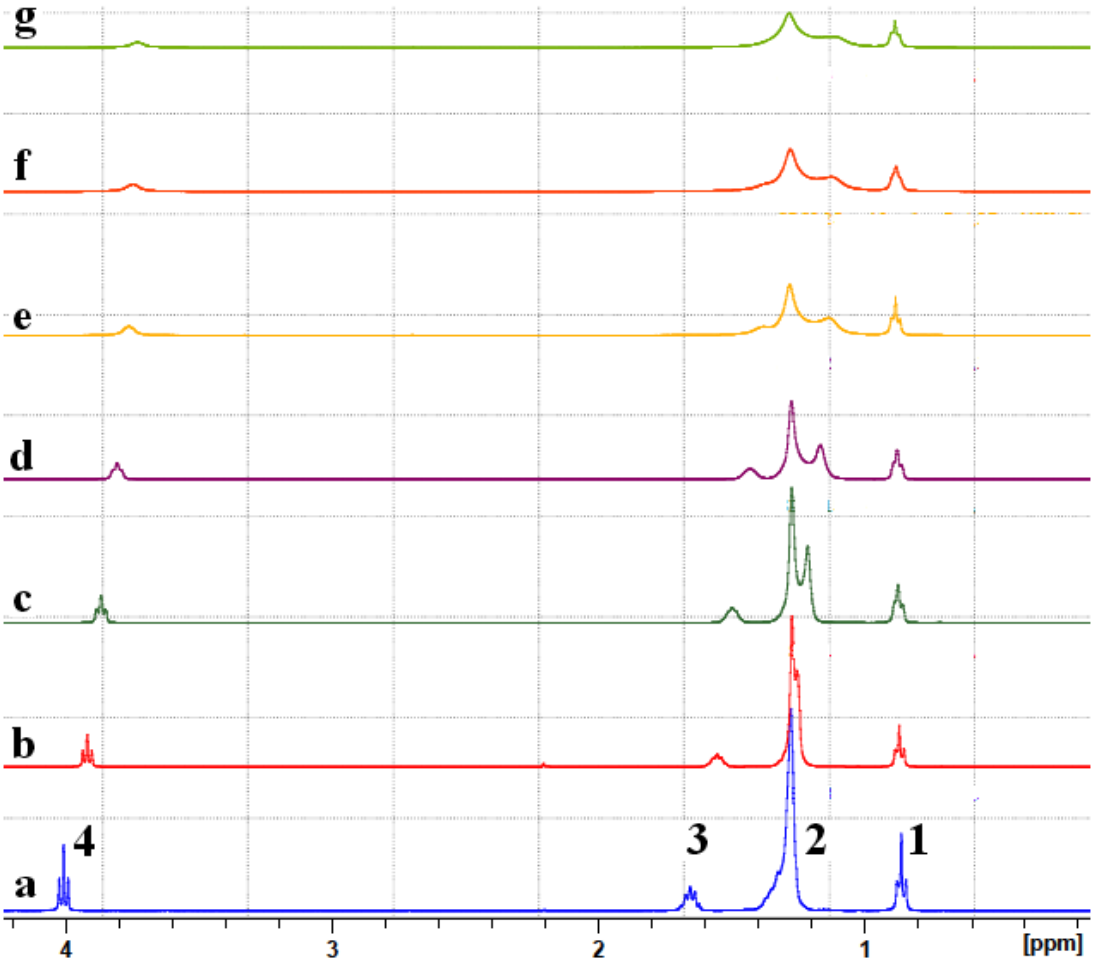

Figure 14 ^{1}H NMR spectra of aqueous 30 mM SDS with various [ANHC] (a) pure 30 mM SDS (b) 30 mM SDS + 10 mM ANHC (c) 30 mM SDS + 15 mM ANHC (d) 30 mM SDS + 20 mM ANHC (e) 30 mM SDS + 25 mM ANHC (f) 30 mM SDS + 30 mM ANHC (g) 30 mM SDS + 35 mM ANHC at 30 $^{\circ}$C.

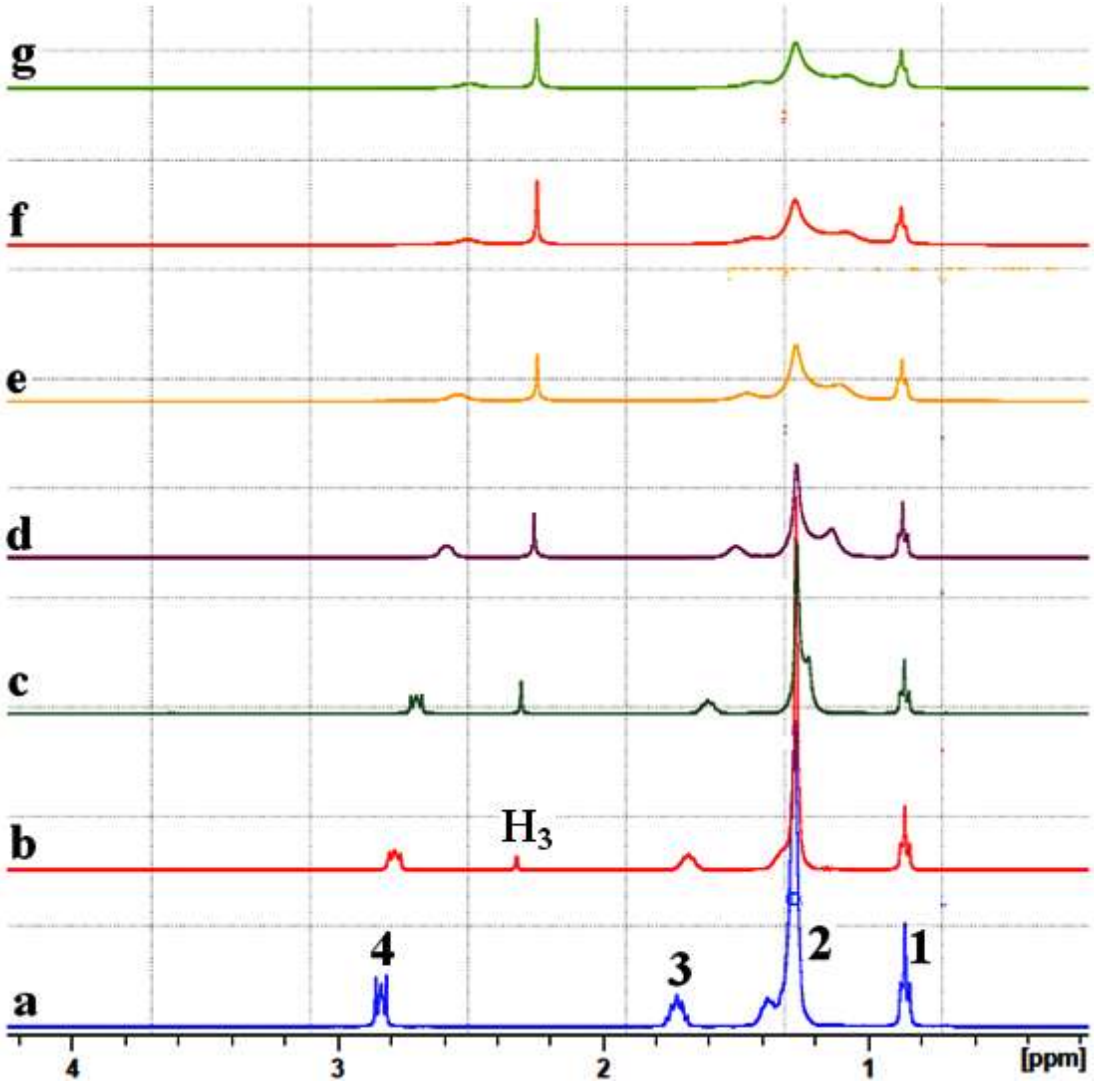

Figure 15 ^{1}H NMR spectra of aqueous 30 mM SDST with various [PTHC] (a) pure 30 mM SDST (b) 30 mM SDST + 5 mM PTHC (c) 30 mM SDST + 10 mM PTHC (d) 30 mM SDST + 15 mM PTHC (e) 30 mM SDST + 20 mM PTHC (f) 30 mM SDST + 25 mM PTHC (g) 30 mM SDST + 30 mM PTHC at 30 $^{\circ}$C (H_3 belongs to PTHC).

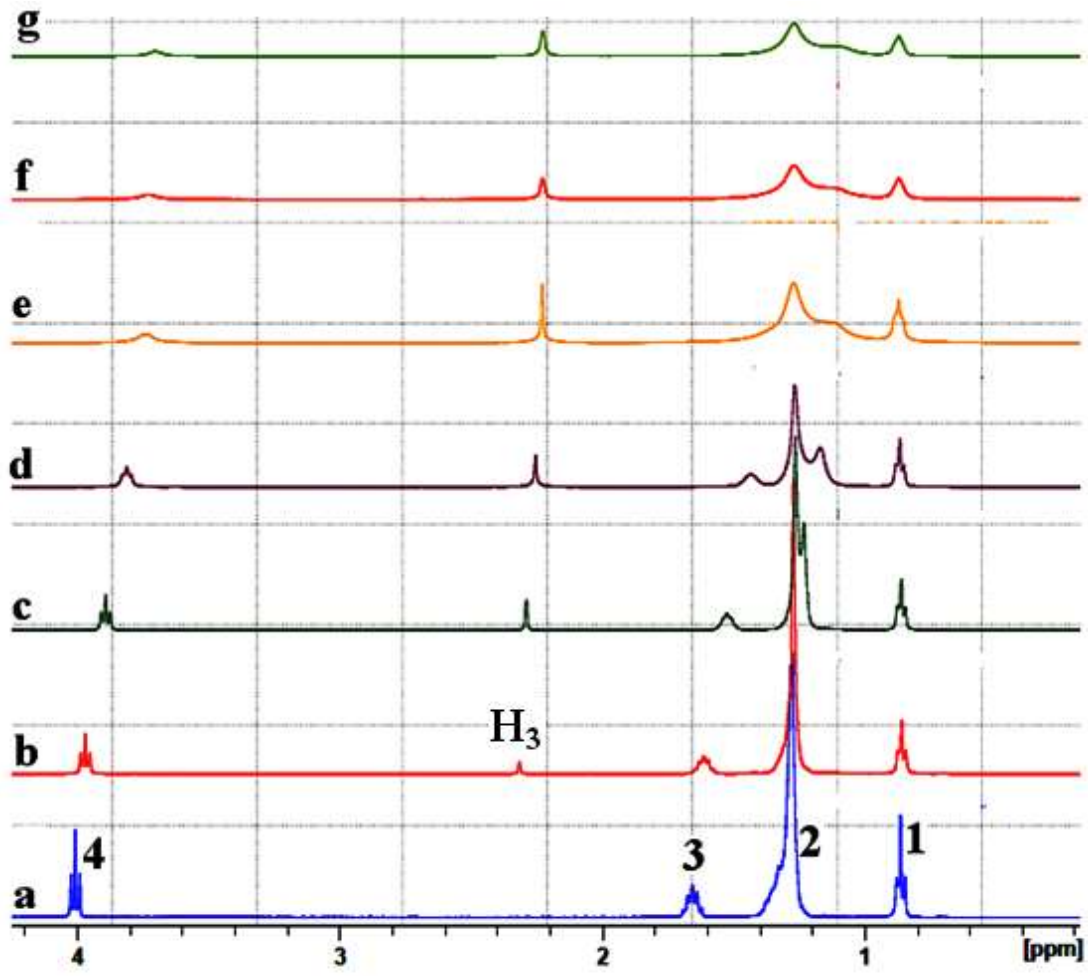

Figure 16 ^{1}H NMR spectra of aqueous 30 mM SDS with various [PTHC] (a) pure 30 mM SDS (b) 30 mM SDS + 5 mM PTHC (c) 30 mM SDS + 10 mM PTHC (d) 30 mM SDS + 15 mM PTHC (e) 30 mM SDS + 20 mM PTHC (f) 30 mM SDS + 25 mM PTHC (g) 30 mM SDS + 30 mM PTHC at 30 $^{\circ}$C (H_3 belongs to PTHC).

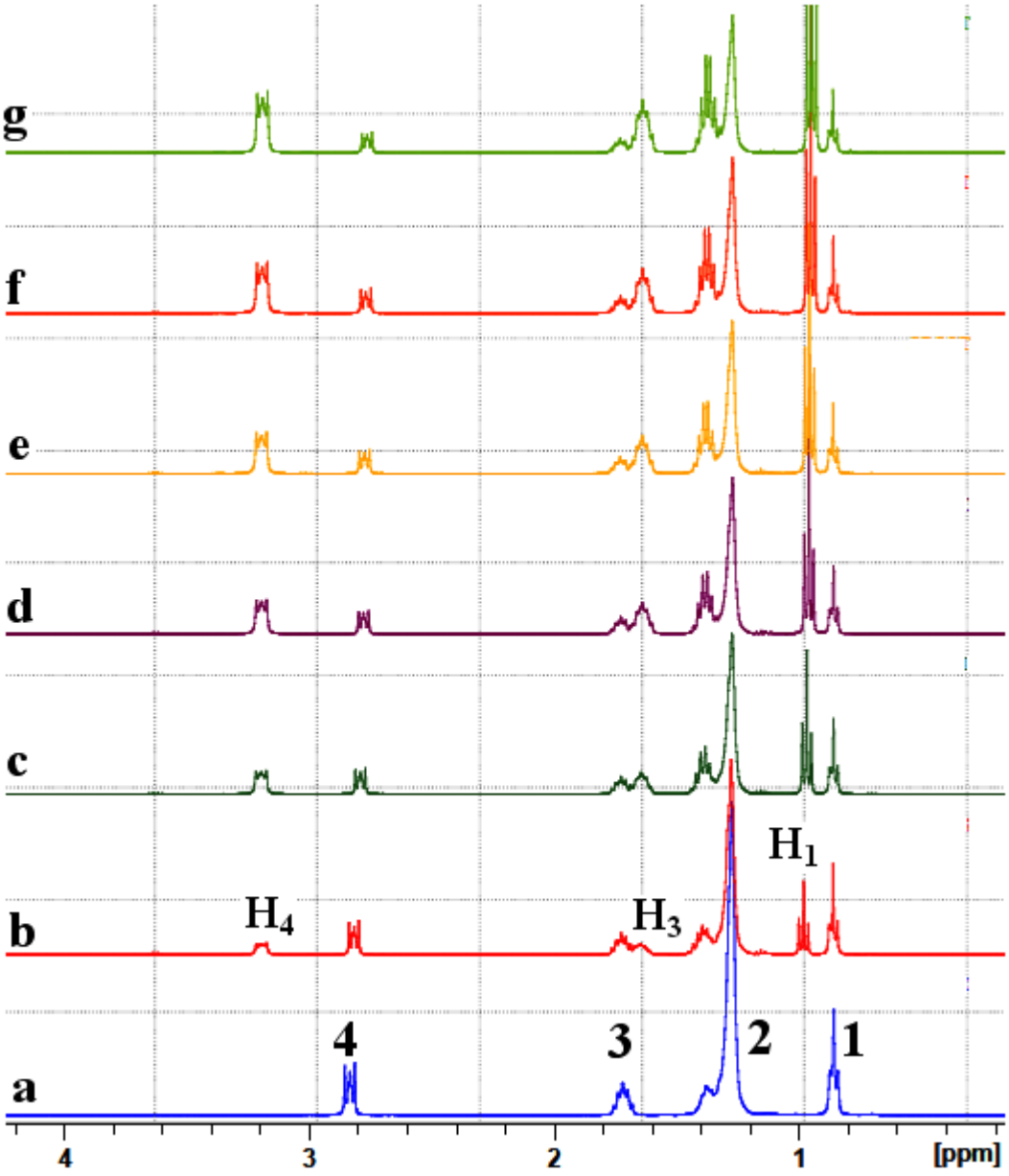

Figure 17 ^{1}H NMR spectra of aqueous 30 mM SDST with various [TBAB] (a) pure 30 mM SDST (b) 30 mM SDST + 5 mM TBAB (c) 30 mM SDST + 10 mM TBAB (d) 30 mM SDST + 15 mM TBAB (e) 30 mM SDST + 20 mM TBAB (f) 30 mM SDST + 25 mM TBAB (g) 30 mM SDST + 30 mM TBAB at 30 $^{\circ}$C (H_3 and H_4 belong to TBAB).

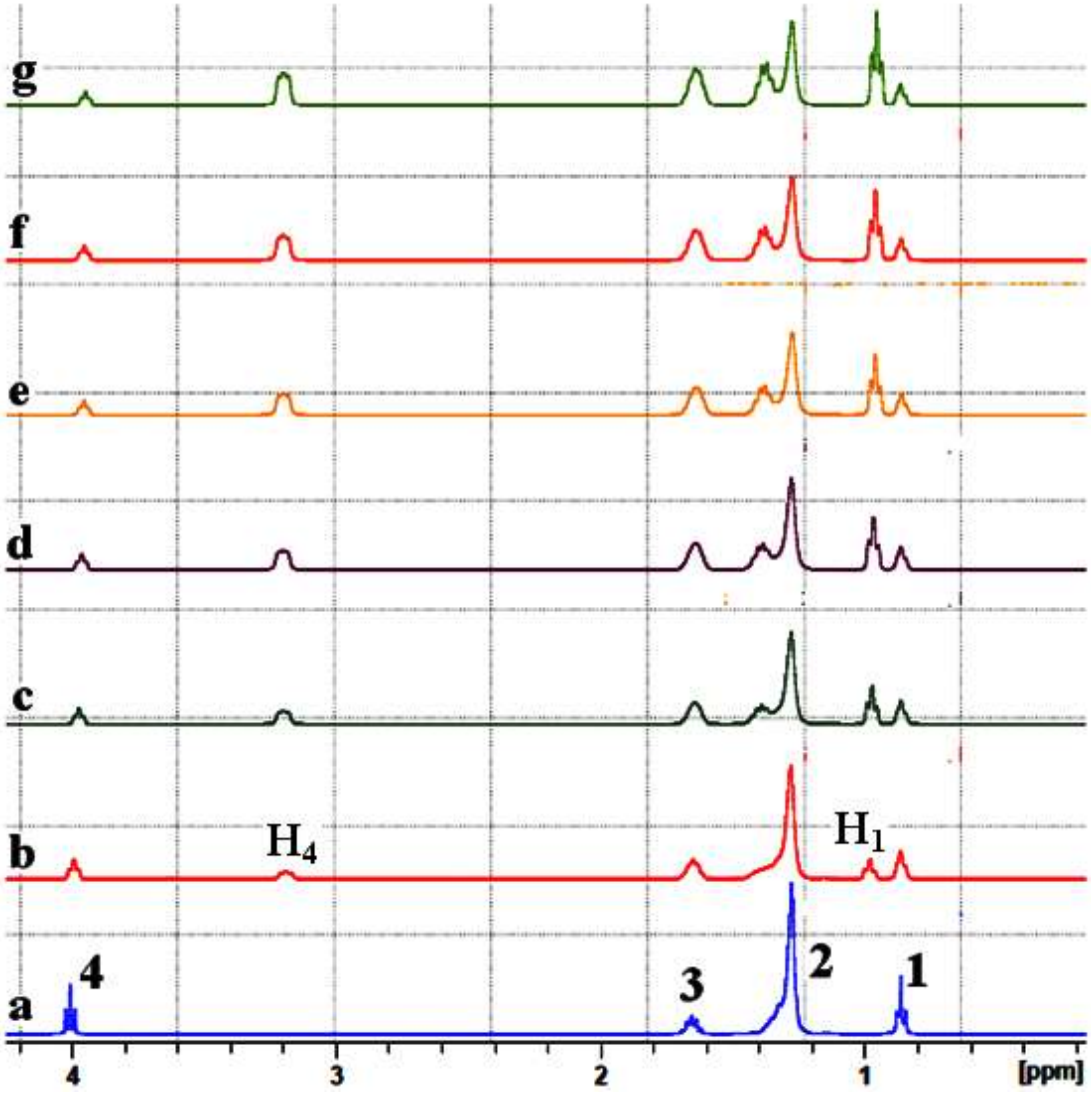

Figure 18 ^{1}H NMR spectra of aqueous 30 mM SDS with various [TBAB] (a) pure 30 mM SDS (b) 30 mM SDS + 5 mM TBAB (c) 30 mM SDS + 10 mM TBAB (d) 30 mM SDS + 15 mM TBAB (e) 30 mM SDS + 20 mM TBAB (f) 30 mM SDS + 25 mM TBAB (g) 30 mM SDS + 30 mM TBAB at 30 $^{\circ}$C (H_3 and H_4 belong to TBAB).

^{1}H NMR chemical shifts of 30 mM surfactant with different concentration of salts are given in Table 1. In each case, with an increase in [salt], δ values for different protons of surfactant change different to different extent. The increase in δ value for proton of micellar core carbon atom (1-H) and a decrease for protons of carbon atoms near the sulfonate / sulfate head group (2-H, 3-H, 4-H) indicate that interaction between different charged moieties at the micellar surface.

This interaction would lead to compensation of negative charge on SO_3^- / SO_4^-, thereby, reducing its tendency to withdraw electrons from the carbon atoms attached to it. Such protons would get more shielded and show upfield chemical shift. This is very well observed in all resonances of 3-H and 4-H protons of both the surfactants with ANHC/PTHC.

Above observations allow to say that SDS micelles grow significantly on addition of ANHC or PTHC. Among these two salts, PTHC is more effective in changing the δ value and hence the micellar growth phenomenon. Due to the presence of additional methyl group in PTHC, it can penetrate the anionic micelle deeper with a increased influence on interior protons [22]. This can be seen from the variation in δ values of various protons of added salts (Tables 2 and 3). Here, again shift in H_3 proton of PTHC is significant hinting for increased interactions with anionic micelles. The interior penetration of PTHC causes increased hydrophobic interaction and responsible for increased micellar growth compared to other salts.

Table 1. ^{1}H NMR chemical shift (δ, ppm) of SDST/ SDS (30 mM) with various concentrations of additives at 30 ˚C (**A** = 3 merges with 2, **B**= peak disappear).

		δ (ppm) of SDST				δ (ppm) of SDS			
Salt	[Salt] (mM)	1	2	3	4	1	2	3	4
ANHC	0	0.86	1.32	1.72	2.83	0.86	1.30	1.64	4.00
	5	0.86	1.29	1.66	2.77	-	-	-	-
	10	0.87	1.26	1.62	2.72	0.86	1.26	1.55	3.91
	15	0.87	1.25	1.59	2.67	0.86	1.24	1.50	3.86
	20	0.87	1.22	1.53	2.63	0.87	1.22	A	3.80
	25	-	-	-	-	0.88	1.21	B	3.76
	30	-	-	-	-	0.88	1.20	B	3.74
PTHC	5	0.86	1.27	1.72	2.78	0.85	1.27	1.60	3.96
	10	0.86	1.24	1.66	2.70	0.85	1.24	1.52	3.89
	15	0.86	1.20	1.59	2.58	0.86	1.21	A	3.81
	20	0.87	1.19	1.49	2.54	0.87	1.18	B	3.73
	25	0.87	1.17	A	2.50	0.87	1.26	B	3.72
	30	0.87	1.17	A	2.50	0.87	1.26	B	3.70
TBAB	5	0.86	1.28	1.73	2.82	0.85	1.28	1.65	3.99
	10	0.86	1.27	1.72	2.79	0.86	1.27	1.64	3.97
	15	0.86	1.27	1.72	2.78	0.86	1.27	1.64	3.95
	20	0.86	1.27	1.73	2.77	0.86	1.27	1.64	3.95
	25	0.86	1.27	1.73	2.76	0.86	1.27	1.63	3.95
	30	0.86	1.27	1.73	2.76	0.85	1.27	1.64	3.95

Table 2. ^{1}H NMR chemical shifts (δ, ppm) of various concentrations of salt in presence of 30 mM SDST at 30 ˚C.

[Salt](mM)	δ of ANHC		δ of PTHC			δ of TBAB			
	H_1	H_2	H_1	H_2	H_3	H_1	H_2	H_3	H_4
5	7.41	7.30	7.28	7.20	2.32	0.98	1.39	1.65	3.19
10	7.42	7.29	-	-	-	0.97	1.39	1.64	3.20
15	7.38	7.28	7.28	7.12	2.26	0.96	1.38	1.64	3.20
20	7.40	7.30	7.27	7.13	2.24	0.96	1.37	1.64	3.20
25	-	-	7.27	7.13	2.25	0.96	1.38	1.64	3.20
30	-	-	7.27	7.14	2.26	0.95	1.37	1.64	3.20

Table 3 ^{1}H NMR chemical shifts (δ, ppm) of various concentrations of salt in presence of 30 mM SDS at 30 ˚C.

[Salt](mM)	δ of ANHC		δ of PTHC			δ of TBAB			
	H_1	H_2	H_1	H_2	H_3	H_1	H_2	H_3	H_4
5	-	-	7.24	7.18	2.31	0.98	1.39	1.65	3.19
10	7.40	7.28	7.26	7.16	2.28	0.97	1.39	1.64	3.20
15	7.41	7.29	7.26	7.11	2.25	0.96	1.38	1.64	3.20
20	7.39	7.28	7.26	7.10	2.22	0.96	1.37	1.64	3.20
25	7.39	7.27	7.26	7.12	2.24	0.96	1.38	1.64	3.20
30	7.39	7.28	7.26	7.12	2.24	0.95	1.37	1.64	3.20

Figures 19 -22 show the NMR spectra of various surfactant-drug combinations. The observed chemical shifts for various combinations are given in Tables 4. As discussed about viscosity increase in case of SDS-PMZ, NMR spectra and δ value results also supporting the discussion made about micellar growth. However, drugs are having bulkier structures (Scheme1 of chapter 2) than above organic salts. They also have more hydrophobic volume which will assist in hydrophobic interactions. This has been reflected from the NMR results where peak broadening /disappearance started at quite lower [drug]. Among the drugs, PMZ was found more effective in influencing the NMR of both the surfactants. It seems that lower molecular area of PMZ allows it to interact with protons near the headgroup region. Further, presence of hetero atoms in the middle ring of PMZ may provide a polar character which can assist PMZ to remain in the micellar surface region and to influence protons near the micellar surface. This indeed was observed even from the δ value variations of both the drugs in presence of surfactants (Tables 5 and 6).

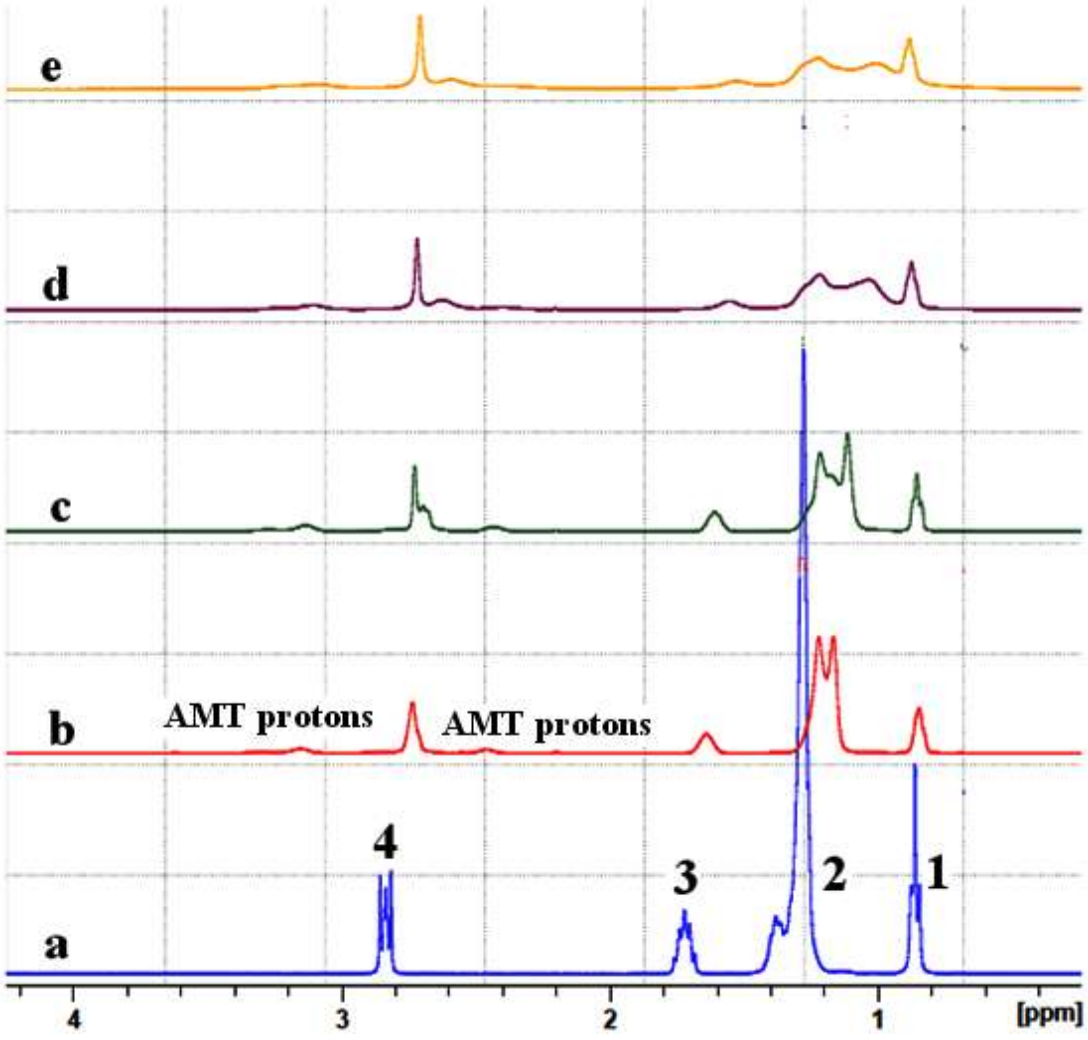

Figure 19 ^{1}H NMR spectra of aqueous 30 mM SDST with various [AMT] (a) pure 30 mM SDST (b) 30 mM SDST + 5 mM AMT (c) 30 mM SDST + 7 mM AMT (d) 30 mM SDST + 10 mM AMT (e) 30 mM SDST + 12 mM AMT at 30 $^{\circ}$C.

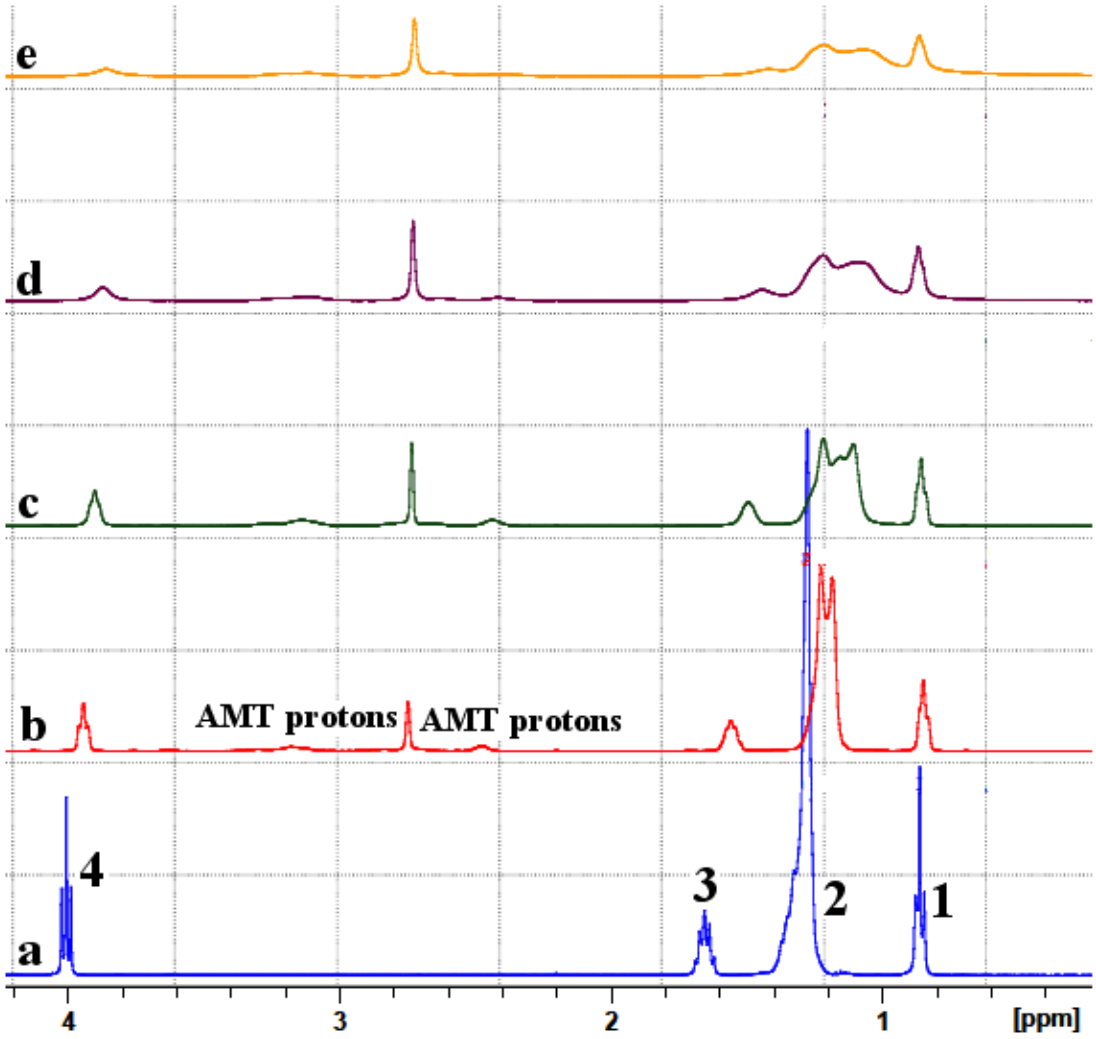

Figure 20 ^{1}H NMR spectra of aqueous 30 mM SDS with various [AMT] (a) pure 30 mM SDS (b) 30 mM SDS + 5 mM AMT (c) 30 mM SDS + 7 mM AMT (d) 30 mM SDS + 10 mM AMT (e) 30 mM SDS + 11 mM AMT at 30 $^{\circ}$C.

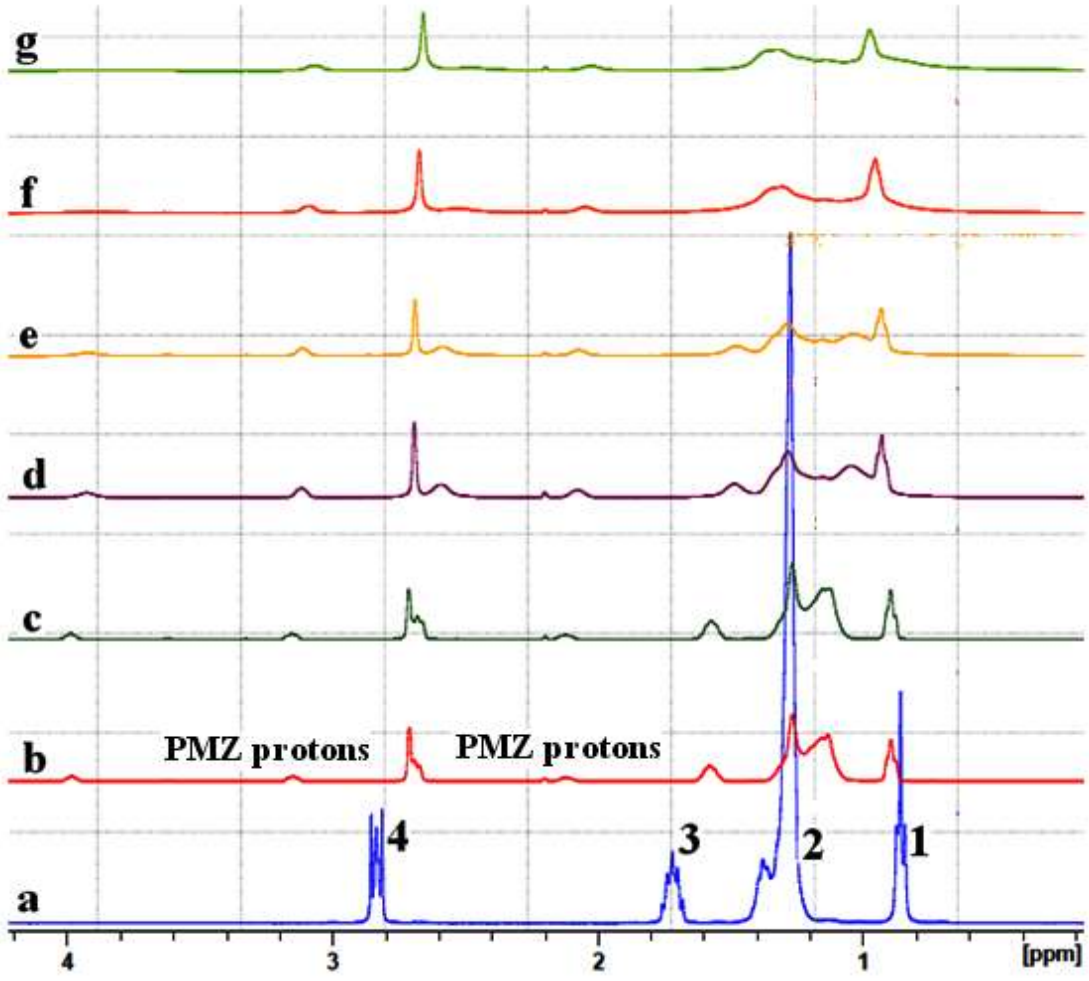

Figure 21 ^{1}H NMR spectra of aqueous 30 mM SDST with various [PMZ] (a) pure 30 mM SDST (b) 30 mM SDST + 5 mM PMZ (c) 30 mM SDST + 7 mM PMZ (d) 30 mM SDST + 10 mM PMZ (e) 30 mM SDST + 12 mM PMZ (f) 30 mM SDST + 15 mM PMZ (g) 30 mM SDST + 17 mM PMZ at 30 $^{\circ}$C.

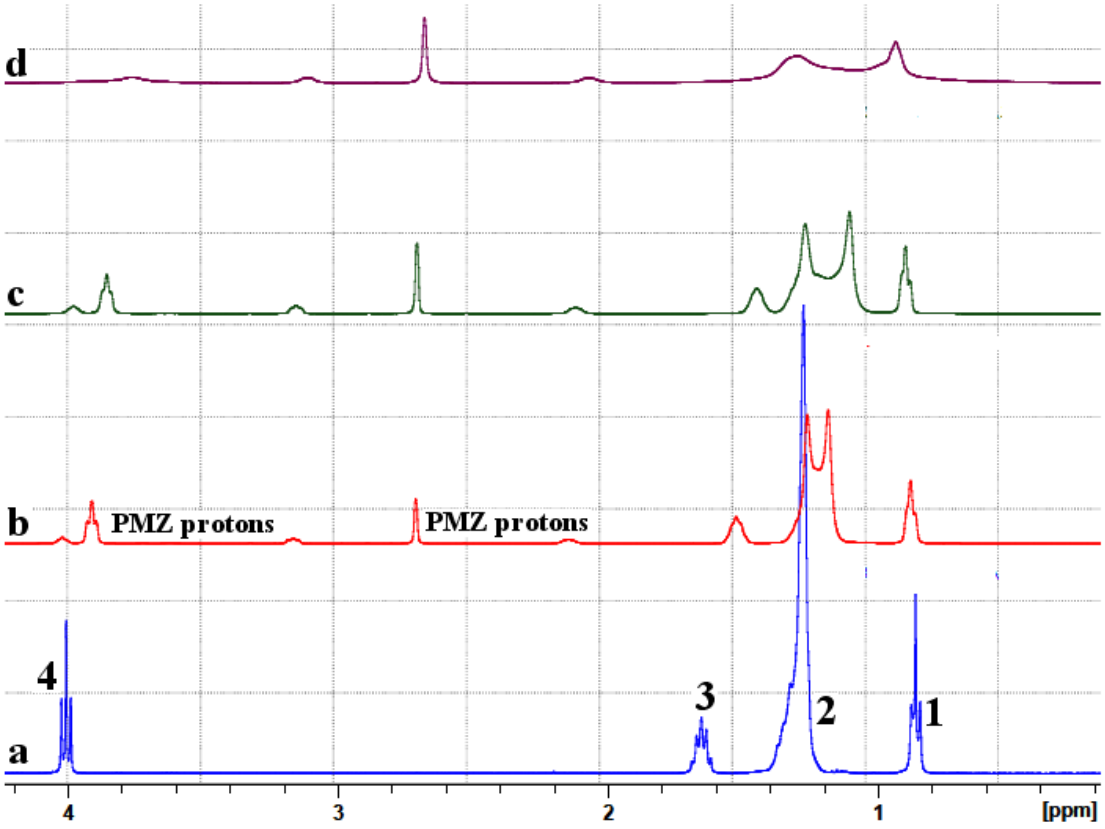

Figure 22 ^{1}H NMR spectra of aqueous 30 mM SDS with various [PMZ] (a) pure 30 mM SDS (b) 30 mM SDS + 5 mM PMZ (c) 30 mM SDS + 7 mM PMZ (d) 30 mM SDS + 10 mM PMZ (e) 30 mM SDS + 13 mM PMZ at 30 $^{\circ}$C.

Table 4. ^{1}H NMR chemical shift (δ, ppm) of SDST/ SDS (30 mM) with various concentrations of drug at 30 ˚C.

Drug	[Drug]	δ (ppm) of SDST				δ (ppm) of SDS			
	(mM)	1	2	3	4	1	2	3	4
	0	0.86	1.32	1.72	2.83	0.86	1.30	1.64	4.00
AMT	5	0.84	1.19	1.63	2.73	0.84	1.20	1.60	3.94
	7	0.84	1.16	1.60	2.70	0.85	1.16	1.49	3.90
	10	0.87	C	A	2.67	0.86	C	A	3.87
	11	-	-	-	-	0.86	C	A	3.86
	12	0.88	C	A	2.65	-	-	-	-
PMZ	5	0.89	1.18	1.58	2.69	0.87	1.22	1.53	3.89
	7	0.89	1.18	1.57	2.68	0.87	1.22	1.52	3.89
	10	0.93	C	A	2.63	0.89	1.18	1.50	3.85
	12	0.93	C	A	2.63	-	-	-	-
	13	-	-	-	-	0.93	C	B	3.76
	15	0.95	C	B	2.60	-	-	-	-
	17	0.97	C	B	2.57	-	-	-	-

A = 3 merges with 2, B= peak disappear, C= 2 merges with1

Table 5 ^{1}H NMR chemical shifts (δ, ppm) of AMT/PMZ with 30 mM SDST at 30 ˚C.

[Drug](mM)	δ of AMT	δ of PMZ[a]						
	Aromatic protons	H_1	H_2/ H_3	H_4	H_5	H_6	H_7	H_8
5	7.08	7.17	6.99	6.82	3.98	3.15	2.71	2.12
7	7.03	7.17	6.99	6.82	3.98	3.15	2.71	2.12
10	7.01	7.12	6.94	6.75	3.92	3.11	2.69	2.07
12	7.01	7.12	6.95	6.74	3.92	3.11	2.69	2.07
15	-	7.09	6.91	6.71	3.89	3.09	2.67	2.05
17	-	7.08	6.89	6.70	3.86	3.06	2.66	2.02

[a] H_1 / H_2 and H_3 / H_4 peaks appear together in pure PMZ at δ values 7.29 ppm and 7.065 ppm respectively.

Table 6 ^{1}H NMR chemical shifts (δ, ppm) of AMT/PMZ with 30 mM SDS at 30 ˚C.

[Drug](mM)	δ of AMT	δ of PMZ						
	Aromatic protons	H_1	H_2/ H_3	H_4	H_5	H_6	H_7	H_8
5	7.10	7.19	7.03	6.87	4.03	3.17	2.72	2.15
7	7.06	7.19	7.03	6.86	4.02	3.16	2.71	2.14
10	7.04	7.16	6.99	6.80	3.98	3.15	2.70	2.12
11	7.04	-	-	-	-	-	-	-
13	-	7.11	6.93	6.73	3.76	3.11	2.68	2.06

To corroborate the preposition based on viscosity and NMR results, DLS experiments were performed with various systems at different additive concentrations. In most of the cases, two populations of association structures are observed (Figures 23-27). However, with increase in [salt] / [drug], each population shows a distinct increase in average size (NNLS analysis). This indicates that DLS data are in conformity to viscosity and NMR results.

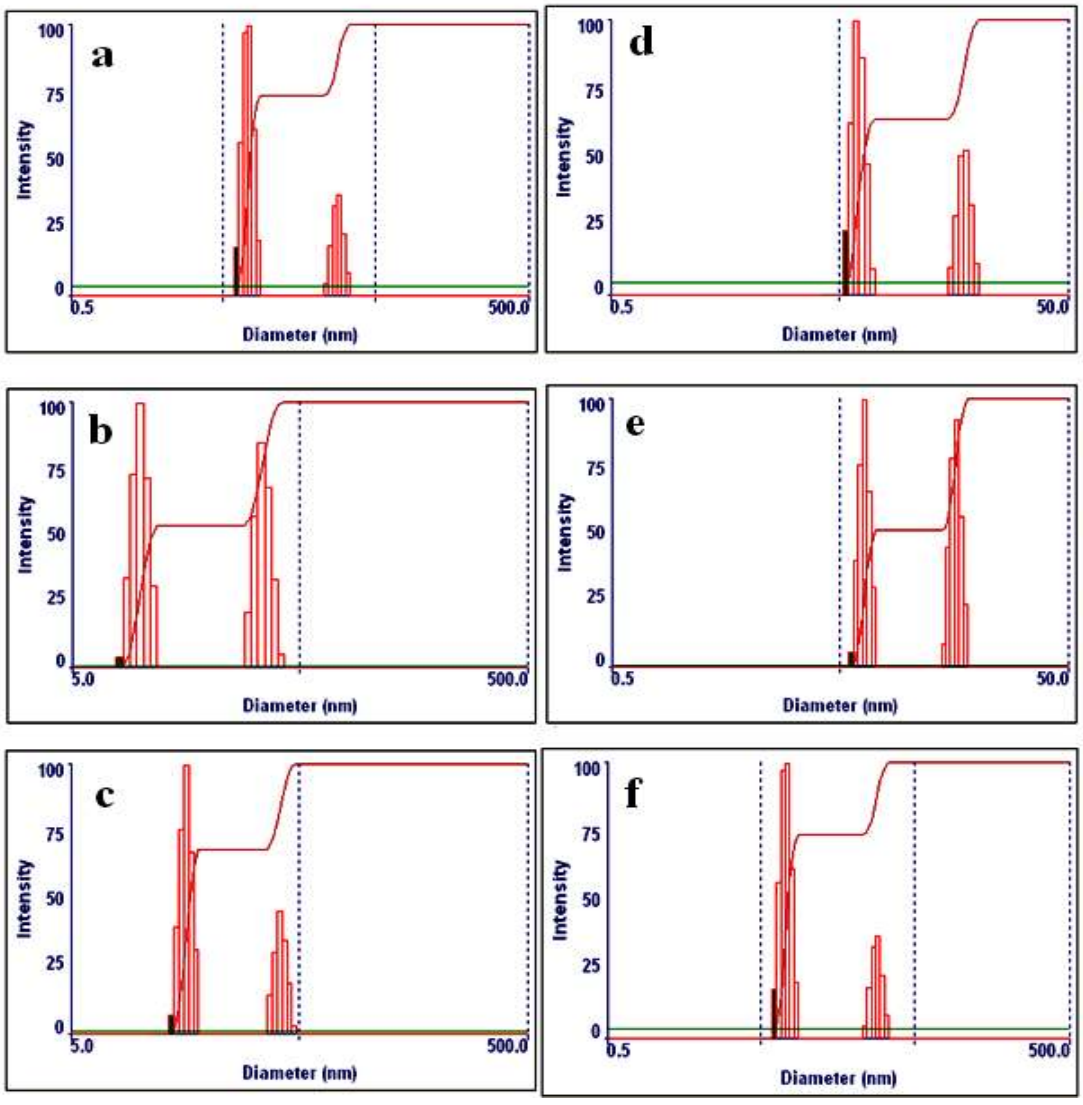

Figure 23 Size distribution profile of aggregates of aqueous 30 mM SDS/SDST with different concentration of ANHC at 30 ^{o}C (a) 30 mM SDS + 5 mM ANHC (b) 30 mM SDS + 20 mM ANHC (c) 30 mM SDS + 30 mM ANHC (d) 30 mM SDST+ 5 mM ANHC (e) 30 mM SDST+ 15 mM ANHC (f) 30 mM SDST+ 20 mM ANHC.

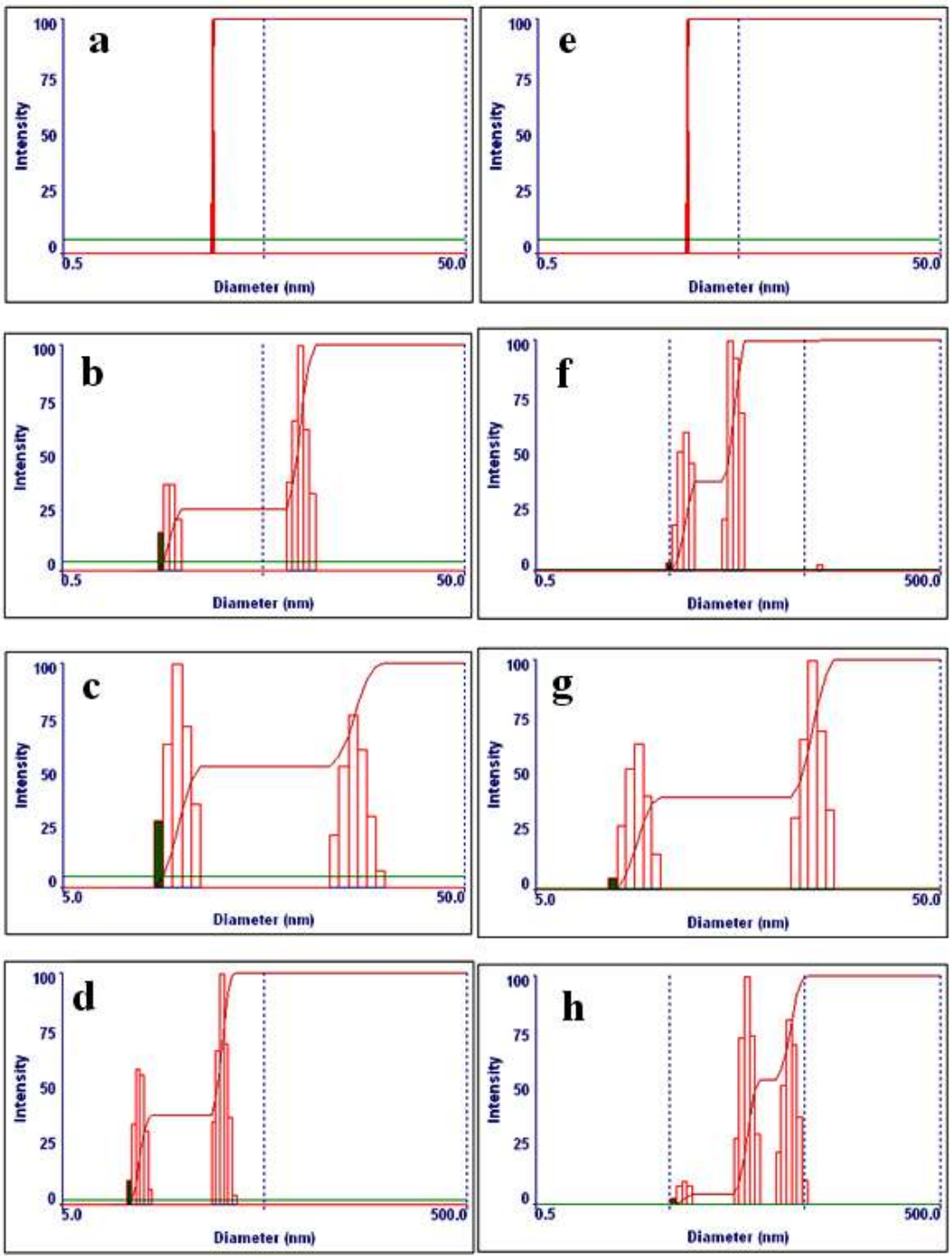

Figure 24 Size distribution profile of aggregates of aqueous 30 mM SDS/SDST with different concentration of PTHC at 30 ^{o}C (a) 30 mM SDST + 5 mM PTHC (b) 30 mM SDST + 15 mM PTHC (c) 30 mM SDST + 20 mM PTHC (d) 30 mM SDST + 30 mM PTHC (e) 30 mM SDS+ 5 mM PTHC (f) 30 mM SDS+ 15 mM PTHC (g) 30 mM SDS+ 20 mM PTHC (h) 30 mM SDS+ 30 mM PTHC.

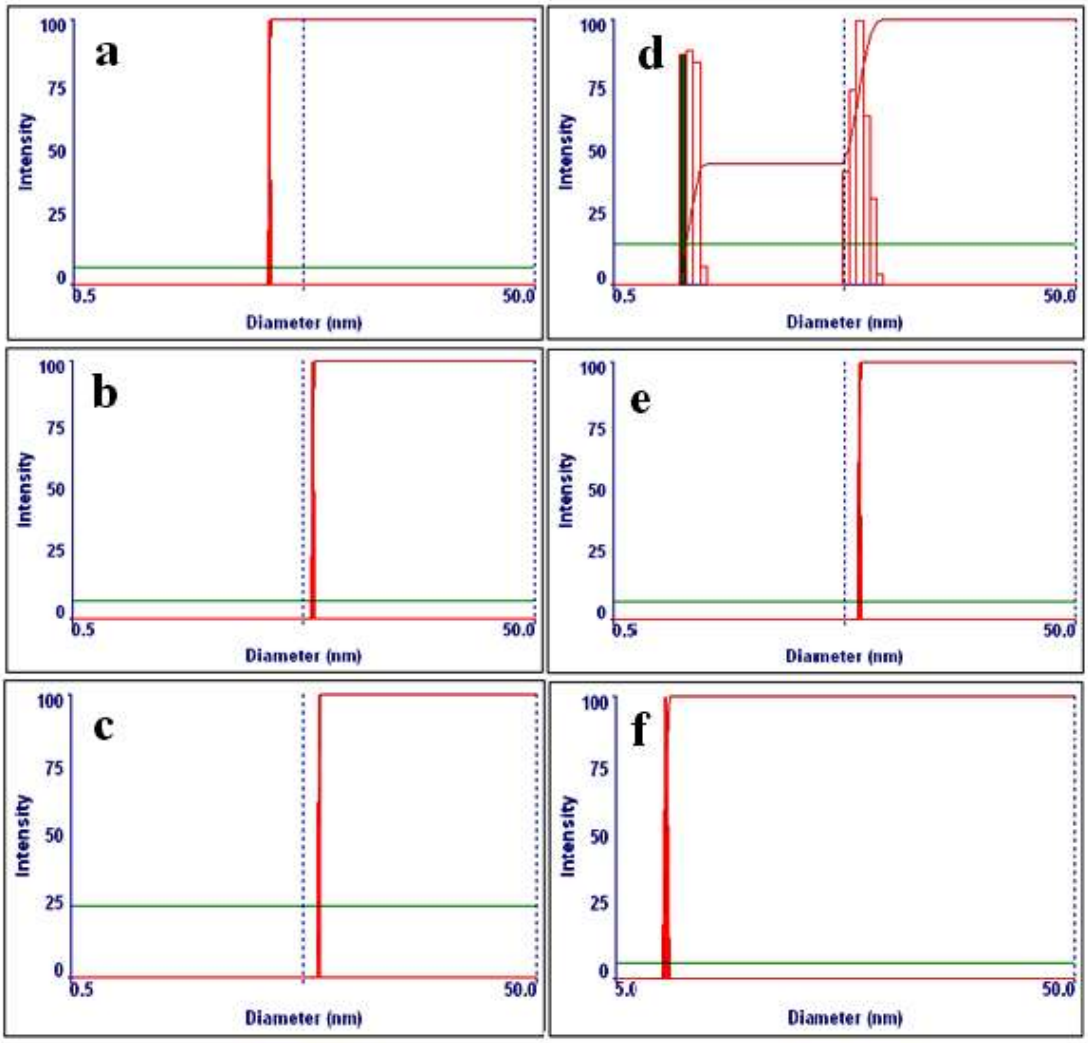

Figure 25 Size distribution profile of aggregates of aqueous 30 mM SDS/SDST with different concentration of TBAB at 30 ^{o}C (a) 30 mM SDST + 5 mM TBAB (b) 30 mM SDST + 15 mM TBAB (c) 30 mM SDST + 30 mM TBAB (d) 30 mM SDS+ 5 mM TBAB (e) 30 mM SDS+ 15 mM TBAB (f) 30 mM SDS+ 30 mM TBAB.

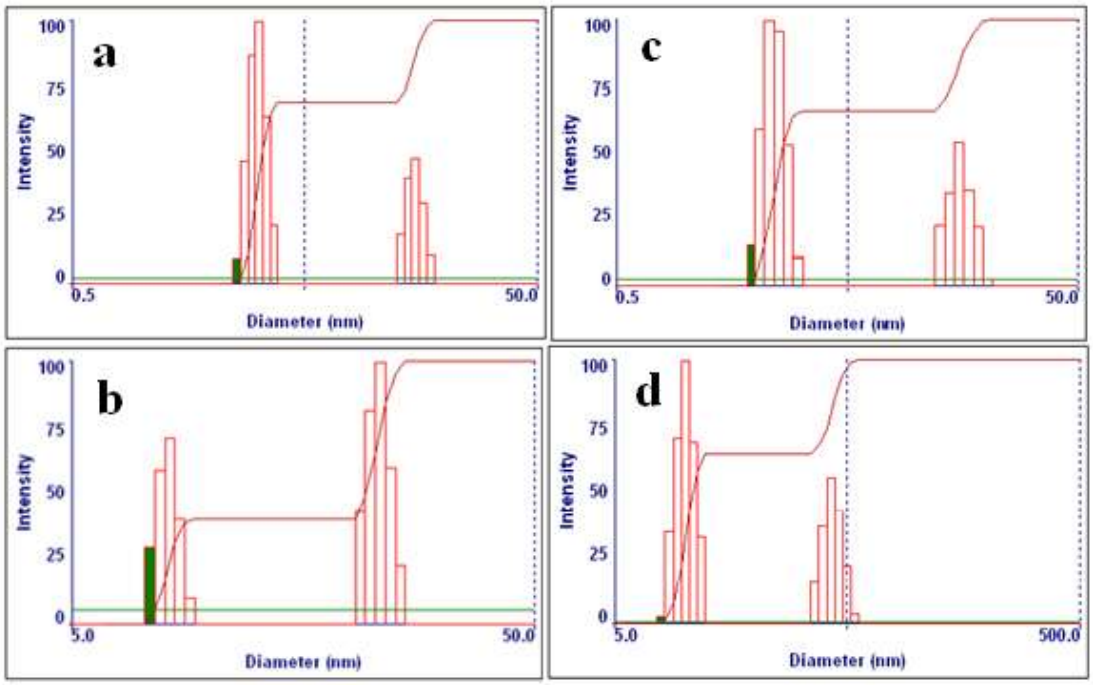

Figure 26 Size distribution profile of aggregates of aqueous 30 mM SDS/SDST with different concentration of AMT at 30 ^{o}C (a) 30 mM SDST + 5 mM AMT (b) 30 mM SDST + 10 mM AMT (c) 30 mM SDS + 5 mM AMT (d) 30 mM SDS+ 10 mM AMT.

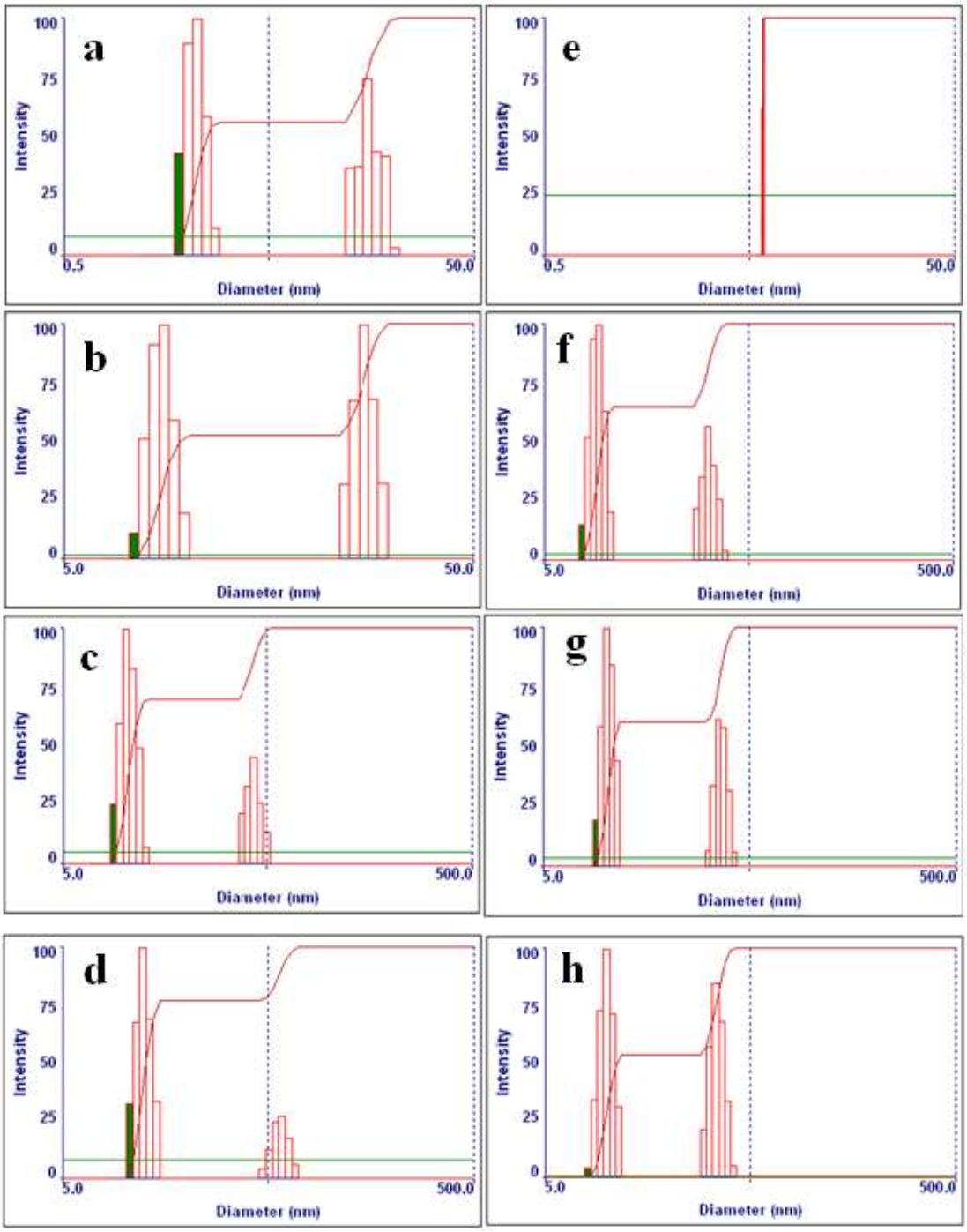

Figure 27 Size distribution profile of aggregates of aqueous 30 mM SDS/SDST with different concentration of PMZ at 30 ^{o}C (a) 30 mM SDST + 5 mM PMZ (b) 30 mM SDST + 10 mM PMZ (c) 30 mM SDST + 12 mM PMZ (d) 30 mM SDST + 15 mM PMZ (e) 30 mM SDS+ 5 mM PMZ (e) 30 mM SDS+ 7 mM SDS (f) 30 mM SDS+ 10 mM PMZ (g) 30 mM SDS+ 13 mM PMZ.

6.3 Conclusions

Studies in this chapter are performed with the aim of getting micellar growth in anionic surfactant solutions in presence of additives. Results show that SDS is more effective than SDST. With regard of an additive, drugs have been found more effective than organic salts. Probably, hydrophobic volume of an additive plays a role to decide the overall micellar morphology. However, AMT has been found more effective with SDS while PMZ shows its effectiveness with SDST. The extent of penetration / intercalation of an additive depends on substituent on the aromatic ring and ratio of polar to nonpolar structure of the additive and hence its ability of micellar growth.

References

1) J. Yang, *Curr. Opin. Colloid Interface Sci.*7 (2002) 276.
2) G. C. Maitland, *Curr. Opin. Colloid Interface Sci.*5 (2000) 301.
3) H. Rehage, and H. Hoffmann, *J. Phys. Chem.* 92 (1988) 4712.
4) C. Manohar, U. R. K. Rao, B. S. Valaulikar, R. M. Iyer, *J. Chem. Soc., Chem. Commun.*379 (1986).
5) M. E. Cates, *Macromolecules* 20 (1987) 2289.
6) T. Shikata, H. Hirata, T. Kotaka, *Langmuir* 5 (1989) 398.
7) H. Rehage, H. Hoffman, *Mol. Phys.* 74 (1991) 933.
8) K. Bijma, J. B. F. N. Engberts, *Langmuir* 13 (1997) 4843.
9) S. Imai, T. Shikata, *J. Colloid Interface Sci.* 244 (2001) 399.
10) Kabir-ud-Din, S. Kumar, D. Sharma, *J. Surfact. Deterg.*5 (2002) 131.
11) Kabir-ud-Din, W. Fatma, Z. A. Khan, A. A. Dar, *J. Phys. Chem. B* 111 (2007) 8860.
12) L. Wattebled, A. Laschewsky, *Langmuir* 23 (2007) 10044.
13) U. S. Siddiqui, F. Khan, I. A. Khan, A. A. Dar, Kabir-ud-Din, *J. Colloid Interface Sci.* 355 (2011) 131.
14) Tadros, T. F. *Applied Surfactants: Principles and Applications*; Wiley VCH: Weinheim, 2005.
15) Myers, D. *Surfactants Science and Technology*, 3rd ed.; Wiley-Interscience: Hoboken, NJ, 2006
16) H. Shoji, S. Ikeda, *J. Phys. Chem.*, 84 (1980) 7.
17) P. M. Lindemutht, G. L. Bertrand, *J. Phys. Chem.* 97 (1993) 7769.
18) S. Kumar, S. L. David, V. K. Aswal, P. S. Goyal, Kabir-ud-Din, *Langmuir* 13 (1997) 6461.
19) L. J. Magid, Z. Li, *Langmuir* 16 (2000) 10028.
20) S. Kumar, A. Z. Naqvi, Kabir-ud-Din, *Langmuir* 16 (2000) 5252.
21) S. Kumar, A. Z. Naqvi, Kabir-ud-Din, *Langmuir* 17 (2001) 4787.
22) P. A. Hassan, S. R. Raghavan, E. W. Kaler, *Langmuir* 18 (2002) 2543.
23) K. Nakamura, T. Shikata, *Langmuir* 22 (2006) 9853.
24) Kabir-ud-Din, Z. A. Khan, S. Kumar, T. Ahmad, *Colloid Polym. Sci*. 286

(2008) 335.

25) S. Kumar, D. Sharma, Kabir-ud-Din, *J. Surfact. Deterg* 8 (2005) 247.

26) S. J. Bachofer, U. Simonis, T. A. Nowicki, *J. Phys. Chem.* 95 (1991) 480.

27) P. J. Kreke, L. J. Magid, J. C. Gee, *Langmuir* 12 (1996) 699.

28) S. J. Bachofer, U. Simonis, *Langmuir* 12 (1996) 1744.

29) D. Yu, X. Huang, M. Deng, Y. Lin, L. Jiang, J. Huang, Y. Wang *J. Phys. Chem. B* 114 (2010) 14955.

30) S. Kumar, D. Sharma, G. Ghosh, Kabir-ud-Din, *Langmuir* 21 (2005) 9446.

31) H. H. Kohler, J. Strand *J. Phys. Chem.* 94 (1990) 7628.

32) C. Gamboa, L. Sepulveda, *J. Colloid Interface Sci.* 113 (1986) 566.

33) M. Dahanayake, A. W. Cohen, M. J. Rosen, *J. Phys. Chem.* 90 (1980) 2418.

34) J. H. Lin, W. S. Chen, S. S. Hou, *J. Phys. Chem. B* 117 (2013) 12076.

35) M. S. Alam, A. Z. Naqvi, Kabir-ud-Din *J. Chem. Eng. Data* 52 (2007)1326.

36) M. Tata, V. T. John, Y. Y. Waguespack, G. L. McPherson, *J .Phys. Chem.* 98 (1994) 3809.

37) S. A. A. Rizvi, L. Shi, D. Lundberg, F. M. Menger, *Langmuir* 24 (2008) 673.

38) K. Kalyanasundaram, M. Gratzel, J. K. Thomas, *J. Am. Chem. Soc.* 97 (1975) 3915.

39) S. Kumar, H. Patel, *J. Mol. Liquids*, 190 (2014) 74.